J. Fluid Mech. (1980), *vol.* 100, *part* 1, *pp.* 185–192
Printed in Great Britain

Visualization of the acoustic excitation of a subsonic jet

By S. N. HEAVENS
Whittle Laboratory, University of Cambridge, England†

(Received 19 December 1978 and in revised form 11 February 1980)

The response of a subsonic round jet to internal excitation by an acoustic wave has been examined using flow visualization and noise measurements. The jet was subjected to pulse excitation and to harmonic excitation. In both cases large-scale vortex ring structures were observed in the jet mixing layer. With pulse excitation, interactions between the vortex rings were observed, but no associated noise emission could be detected.

1. Introduction

Recent interest in jet-noise research has centred mainly on two aspects: the role played by large-scale coherent structures in the shear-layer mixing process (Moore 1977; Ffowcs Williams & Kempton 1978) and the effect of acoustic disturbances introduced into the flow upstream of the nozzle exit (Bechert & Pfizenmaier 1975; Munt 1977; Bechert, Michel & Pfizenmaier 1977; Moore 1977; Pinker & Bryce 1977). Excitation of the jet is usually accomplished by means of a pure tone, either from a loudspeaker situated on the axis of the plenum chamber (plane-wave mode) or from a series of loudspeakers distributed around the circumference of the nozzle (Bechert & Pfizenmaier 1977), enabling higher-order modes of forcing to be studied. These experiments indicate that the effects of pure-tone excitation depend considerably on the forcing amplitude and frequency; the essential feature, however, is that the interaction of the sound field with the nozzle flow is a nonlinear scattering process resulting not in amplification of the pure tone but in amplification of the broad-band noise field of the jet. In jet flows at high subsonic velocities the directivity of the broad-band noise field of the jet is weakly influenced by the tone, whereas the directivity of the pure-tone diffraction field is substantially influenced by the flow.

In the experiment described in this paper, the jet was excited either by a transient pulse generated by a spark discharge, or by a harmonic source of comparable strength. The response of the jet to pulse excitation was found to be in the form of large quasi-stable vortex rings, a phenomenon which is well known in laminar jets, but not usually observed at Reynolds numbers in the range 10^5–10^6. It was possible to follow in detail the formation, convection and interaction of the vortex rings and the alteration of the acoustic diffraction field in the presence of flow. A significant increase in noise output was detected from the excited jet, but this could not be attributed to amplification of the sound pulse by the nozzle flow or to interactions between the vortex rings.

† Present address: Chloride Silent Power Limited, Astmoor, Runcorn, Cheshire.

0022-1120/80/4556-2190 $02.00

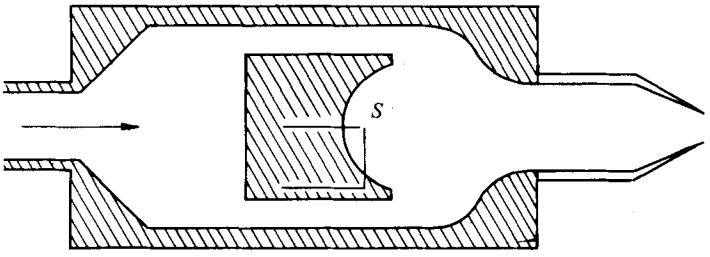

FIGURE 1. Schematic diagram of the nozzle rig used for the study of pulse excitation. S, spark gap. For harmonic excitation the spark-gap assembly was replaced by a transducer horn drive unit.

2. Experimental methods

In the first experiment, the acoustic pulse was generated by a spark discharge of energy 5J. The spark gap was positioned on the axis of a plenum chamber of diameter 0·2 m and length 0·35 m (figure 1). Air was supplied by a 7·5 kW eccentric vane compressor, via a primary settling chamber and through a pipe 50 mm in diameter, to the jet rig which was situated at the centre of an anechoic chamber of dimensions $3 \times 3 \times 2{\cdot}5$ m. The spark gap was positioned at the focus of a paraboloidal reflector of diameter 100 mm in order to generate a strong N wave by reflexion. The nozzle was a cone of semi-angle 15°, with an inlet diameter of 75 mm and an exit diameter of 12·5 mm. A cylindrical nozzle of length 100 mm and diameter 12·5 mm was used in some experiments.

The jet was visualized with a Z-type schlieren system with $f/10$ mirrors of diameter 100 mm. The light source was an argon-jet spark gap of duration 0·2 μs, triggered from the acoustic spark via a variable time delay.

In conjunction with the schlieren photography an attempt was made to obtain measurements of the strength of the diffracted sound pulse. The spark discharge generated an N wave of duration 50 μs and rise time 15 μs; measurements of the pulse could therefore be obtained with a B & K 3 mm microphone, which has a bandwidth of 160 kHz. However, a comparison of pulse measurements made with and without flow could only be made after allowing for the effect of the plenum-chamber stagnation pressure on the acoustic efficiency of the spark gap. For a point spark discharge the acoustic pulse energy E_{ac} is known to depend on gas pressure P_0, density ρ_0 and electrical energy E in the form (Wyber 1975):

$$E_{ac} \sim E_0 \rho_0^{\frac{1}{2}} P^{-\frac{1}{2}}. \tag{1}$$

Since E_0 was kept constant, the acoustic output of the spark discharge decreased as the nozzle pressure ratio was increased. For a pressure ratio of 1·52 (the maximum used in the experiment) the amplitude of the pressure wave from the spark was 0·82 relative to that at zero flow.

In the second experiment, the jet was forced by a high intensity harmonic acoustic field generated by a transducer horn drive unit of diameter 20 mm and frequency 20 kHz. The unit was mounted on the axis of a plenum chamber of diameter 0·15 m and length 0·5 m. Sound pressure measurements of the jet and the 20 kHz diffraction field were made with a B & K 12·5 mm microphone.

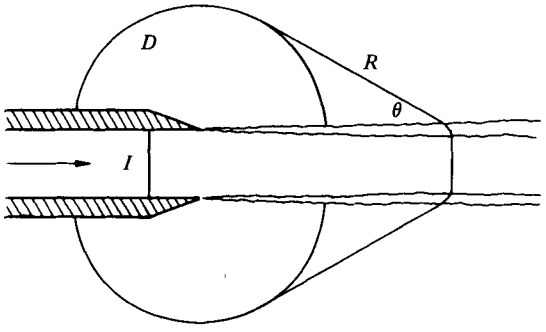

FIGURE 3. Schematic diagram showing the diffraction of a plane sound wave at the nozzle exit. I, incident wave; D, diffracted wave; R, refracted wave, $\sin\theta = (1+M)^{-1}$, where $M = U_0/a_0$ is the nozzle exit Mach number.

3. Excitation by a transient pulse

3.1. *Flow visualization*

The nozzle exit Mach number was varied over the range 0·2–0·8 ($Re = 5\times10^4$ to 2×10^5). A sequence of schlieren photographs taken with the knife edge vertical (parallel to the jet axis) is shown in figure 2 (plate 1). The time scale on the time-delay generator was found to be inaccurate, but it could be calibrated from the photographs, since the velocity of propagation of the acoustic pulse is known. In figures 2 and 4–6 the time interval between successive frames is 33 μs.

Figure 2 shows the response of the Mach 0·6 jet to excitation by the transient pulse from the spark discharge. A series of vortices is formed in the shear layer mixing region, and the sound pulse is diffracted from the nozzle lip and refracted through the shear layer (figure 3). There is a certain amount of confused detail in the photographs resulting from small-scale turbulence in the jet, and from thermal convection in the ambient air. A method of removing these unwanted features, and thereby of highlighting essential details, is the application of a photographic averaging technique developed by Moore (1977), who found this to be an effective method of revealing large-scale structure even in an unforced jet. The method involved the repeated triggering of the light source and superposition of all the schlieren images on a single photographic negative, so that any coherent structure associated with the trigger signal is reinforced, while images from 'random' turbulence tend to cancel out. In figure 4 (plate 2) each frame represents 10 superimposed images triggered at fixed delay from the acoustic spark. The essential features of the interaction process are now seen more clearly. The shedding of vorticity from the nozzle lip is in the form of vortex rings. The N-wave acoustic pulse contains two sharp peaks, both of which are visible in figures 4(*d*) and (*e*). The two peaks generate two large vortex rings, the first of which convects downstream with a velocity equal to $0{\cdot}7U_0$ (where U_0 is the nozzle exit velocity) and diffuses rapidly. The second vortex convects with velocity $0{\cdot}5U_0$ and grows as a result of coalescence with other smaller vortex rings.

Photographs of a Mach 0·8 jet showed sound refraction through a smaller angle θ, a greater tendency for the vortex rings to distort from planar, and an increase in the intensity of the wave diffracted at 90° to the jet axis. With zero flow, diffracted waves were spherical as expected. Visualization of the jet from the cylindrical nozzle indicated weaker vortex-ring development and weaker sound-wave diffraction.

3.2. *Measurement of the diffracted pulse*

Schlieren photographs provide only a qualitative measure of pressure gradient. To obtain quantitative measurements of the diffracted pulse, a B & K 3 mm microphone was placed in the horizontal plane of the nozzle exit, at a radial distance of 40 nozzle diameters. Figure 7 shows oscilloscope records of the diffracted pulse at different jet Mach numbers varying from zero to 0·8. Figure 5(*a*) (see plate 3) shows the N wave in the absence of flow (on all the oscilloscope traces, the direction of increasing pressure is downwards). At low jet velocities there is little effect on the amplitude of the diffracted pulse. The broad-band jet-noise signal is small compared to the acoustic pulse. At higher jet velocities the amplitude of the diffracted pulse increases, in spite of the drop in efficiency of the acoustic source (§ 2).

The origin of the intensification of the diffracted pulse in the presence of flow could not be ascertained, as it was not possible with the present experimental arrangement to make reference microphone measurements upstream of the nozzle exit. However, it is more likely to be due to an increase in the acoustic reflexion coefficient of the nozzle (Bechert *et al.* 1977) than to a genuine amplification of the incident sound pulse by the flow.

Figure 6 (plate 4) shows oscilloscope records obtained from a microphone placed at 45° to the jet axis. In this case the apparent intensification of the N wave in the presence of flow is probably due to refraction of the wave through the jet shear layer.

3.3. *Details of the vortex-ring motion*

In order to visualize in detail the development and interaction of the vortex rings, schlieren photographs were taken with the knife edge horizontal (perpendicular to the jet axis) and the time interval between successive frames was reduced to 15 μs. Figures 7, 8 and 9 (plates 5, 6 and 7) show the vortex-ring development in the jet at nozzle exit Mach numbers equal 0·4, 0·6 and 0·8 respectively. In the Mach 0·4 jet (figure 7) the two large vortices generated by the N wave convect downstream steadily; the first vortex ring diffuses at an axial distance of two diameters from the nozzle, whereas the second vortex ring grows and is quite stable. Other smaller vortices can be seen; these are produced by additional weak pulses from the spark discharge. In the Mach 0·6 jet (figure 8) the vortices are stronger and there is evidence of interaction. As they convect downstream, the earlier vortices diffuse, while the later ones undergo coalescence or 'pairing' with the large vortex ring generated by the rear of the N wave. Vortex pairing is visible in figures 8(*d*), (*e*), (*h*), (*j*) and (*m*). In the Mach 0·8 jet (figure 9) the vortex rings are even stronger and the interaction between them is more violent, resulting in considerable distortion of their ring structure. Vortex pairing events are visible in figures 9(*e*), (*h*), (*i*), (*j*) and (*o*). The vortex annihilation occurring between figures 9(*h*) and (*j*) may be of the type suggested by Moore & Saffman (1975), in which two strong vortices are able to tear apart a weak neighbouring vortex. Figure 10 shows diagrammatically the progress of the series of vortices in figure 7. Figures 11 and 12 are derived in a similar way from figures 8 and 9 respectively. At all jet velocities U_0 the earlier vortex rings convect with velocity $0{\cdot}7U_0$, whereas the later ones convect with velocity $0{\cdot}5U_0$. Instants of vortex coalescence are marked with '*'. The process of coalescence is evidently very rapid. When coalescence occurs between a large and a small vortex, there is little tendency for the

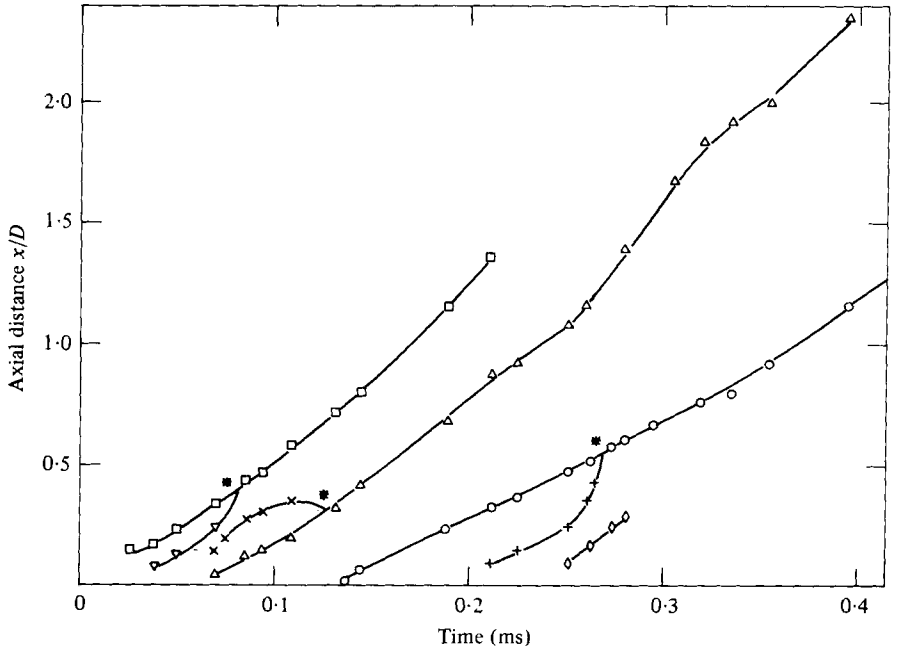

FIGURE 10. Progress of the vortex rings in the excited Mach 0·4 jet. Positions of vortex coalescence are labelled with *.

velocity of the large vortex to be affected; this differs from the observations of Acton (1976). Here the small vortex appears to be sucked rapidly towards the large one.

The appearance of rapidly coalescing vortex rings is of interest in view of the possibility that coalescence plays an important role in the production of jet noise. The theoretical basis for this mechanism has been established (Ffowcs Williams & Kempton 1978) and there is experimental evidence that vortex pairing does occur as a natural process in low-Reynolds-number free shear layers (Winant & Browand 1974). For round jets at high Reynolds number Moore (1977) and Bruun (1977) have deduced the existence of vortex pairing from the disappearance of peaks observed when comparing signals from two probes at different axial positions. It remains to be shown, however, that this deduction is correct.

In the present experiment the vortex ring kinematics are known, and they can be used to interpret the signals received by a near-field microphone probe. Figure 13 (plate 8) shows a series of signals from a 3 mm microphone placed close to the shear layer of a Mach 0·6 jet, at axial stations ranging from the nozzle exit plane to two nozzle diameters downstream. The left-hand part of each signal is the N wave diffracted from the nozzle lip. The right-hand part represents the near-field profile produced by the convection of the vortex rings past the microphone. At axial positions well downstream (figure 13*o*) this latter part of the oscilloscope trace represents the large vortex which persists throughout the later stages of figure 8. On tracing the history of the profile back to its origin, three positions can be found at which a peak is on the point of annihilation (figures 13*e*, *h*, *n*). These axial positions are at 0·5, 0·8 and 1·6 nozzle diameters, which agree moderately well with the positions of vortex coalescence

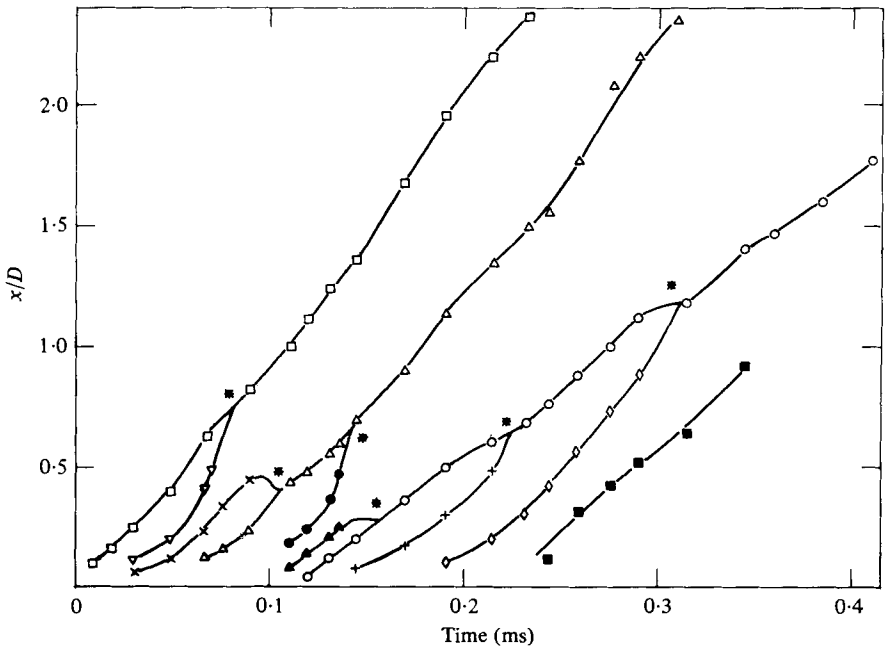

FIGURE 11. Progress of the vortex rings in the excited Mach 0·6 jet.

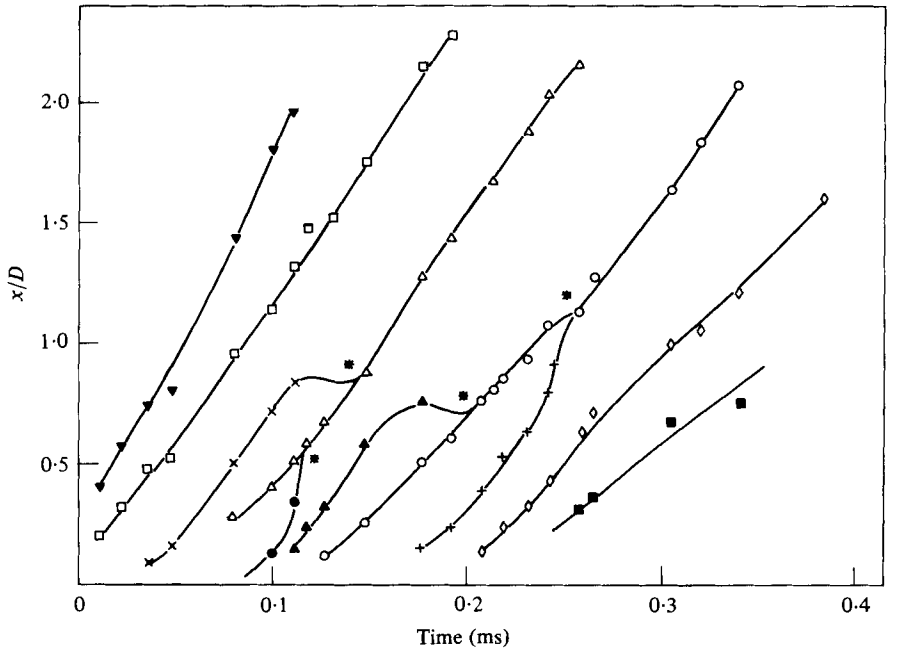

FIGURE 12. Progress of the vortex rings in the excited Mach 0·8 jet.

labelled in figure 11. The agreement is not spectacular, but it is likely that the disappearance of amalgamation of peaks in a near-field microphone signal does represent vortex coalescence.

We now consider whether the experiment provides any indication of far-field sound

Jet Mach no.	Instants of vortex coalescence, relative to the instant that the N wave leaves the nozzle (μs)		
0·4	—	200	—
0·6	—	160	240
0·8	75	135	190

(Only pairings between large vortex rings are listed)

TABLE 1

generation either from the growth and decay of the vortex rings, or from their coalescence. It is conceivable that sound could be generated as a result of any change in form of the vortices as they convect downstream, but the evidence from the photographs suggests that most of the vortex rings are remarkably stable, maintaining their form until they diffuse some 3–5 nozzle diameters downstream of the nozzle exit. It is unlikely that the convection of the vortex rings provides an efficient mechanism for sound generation, it could, however, be responsible for the low-frequency part of the jet noise spectrum, which is comparatively weak.

Vortex coalescence, on the other hand, is a rapid process taking place in times of the order 10 μs. It is of interest to examine the far-field microphone signals for evidence of peaks that could be associated with coalescence. In figure 7 the oscilloscope records obtained at high jet velocities do show the appearance of peaks which are not present in the absence of flow. Close examination indicates, however, that they do not correspond to the instants of vortex pairing observed in the photographs. Furthermore, the positions of the peaks do not change as the jet velocity is varied, whereas it is clear from figures 10–12 that as the jet velocity is reduced, the vortex coalescence events tend to 'spread out' in time (table 1). There is also no evidence of extra noise peaks in the records obtained at 45° to the jet axis (figure 6). It must be concluded that the extra noise measured at 90° to the jet axis results from intensified diffracted pulses and not from vortex coalescence.

Consequently the coalescence of the large vortex rings could not be correlated with any noise peaks distinguishable from the continuous jet noise. According to Ffowcs Williams & Kempton (1978) the pairing of large vortices should be more noisy than the pairing of small ones; however, the contribution from this source may have been too small to detect against the background of the strong acoustic diffraction field.

4. Harmonic excitation of the jet

The experimental arrangement was similar to that shown in figure 1, except that the spark-gap unit was replaced by a Vibrason 300 drive unit with a 20 mm diameter horn, manufactured by Kerry Ultrasonics Limited. The frequency of operation was 20 kHz, corresponding to a Helmholtz number (KR) of 2·3.

The drive unit was mounted on the axis of the plenum chamber, so that the horn radiated an approximately plane wave along the jet axis. The radiating surface of the horn was positioned 25 mm upstream of the nozzle contraction (i.e. 125 mm upstream of the nozzle exit). The peak-to-peak displacement amplitude of the horn was variable over the range 3–50 μm.

Spark photographs of the harmonically forced jet are shown in figure 14 (plate 9). The photographs were triggered at random. Figures 14(*b*), (*c*) and (*d*) show the forced jet at Mach numbers 0·3, 0·45 and 0·6 respectively. Figure 14(*a*) shows an unforced Mach 0·3 jet for comparison. The upper row of photographs was taken with the schlieren knife edge horizontal; the lower row shows corresponding photographs taken with a vertical knife edge. At Mach 0·6 the Strouhal number of excitation was 1·25. It was not safe to operate the jet at higher velocities owing to the risk of damage to the transducer at high pressure ratios.

In the harmonically forced jet the vortex rings showed no evidence of interaction, their convection speed remaining steady at $0{\cdot}47U_0$. The 20 kHz diffraction field can be seen in figures 14(*f*) and (*h*). In the absence of flow the diffraction field was not visible.

Sound level measurements of the harmonically forced jet indicated similar results to those obtained with pulse excitation (§ 3.2). In the presence of flow, an increase in diffraction-field intensity of the order 6 dB was observed at 90° to the jet axis and in the forward arc. As in the case of pulse excitation, this increase was more likely to be the result of a change in the acoustic transmission properties of the nozzle than to an amplification of the sound field by the jet shear layer.

5. Conclusions

When a subsonic jet is excited by a sound wave of moderately large amplitude, interaction between the wave and the nozzle exit flow is manifested by the development of large-scale vortex rings and by the diffraction of the wave from the nozzle tip and refraction through the jet shear layer. In the case of harmonic excitation, the vortex rings convect steadily downstream with velocity $0{\cdot}5U_0$. With pulse excitation, convection velocities varying from $0{\cdot}5$–$0{\cdot}7U_0$ are observed and interaction occurs between the vortex rings, resulting in distortion of the rings and ultimately vortex annihilation or coalescence. If the jet velocity is raised the number of vortex coalescence events increases for a given excitation level. An attempt was made to identify the coalescence events as sources of noise, but this was not successful.

I thank Professor J. E. Ffowcs Williams for helpful discussions, a referee for detailed comments and the Science Research Council for financial support.

REFERENCES

Acton, E. 1976 *J. Fluid Mech.* **76**, 561–582.
Bechert, D., Michel, U. & Pfizenmaier, E. 1977 *A.I.A.A. Paper* 77-1278.
Bechert, D. & Pfizenmaier, E. 1975 *J. Sound Vib.* **43**, 581–587.
Bechert, D. & Pfizenmaier, E. 1977 *A.I.A.A. J.* **15**, 1268–1271.
Bruun, H. 1977 *J. Fluid Mech.* **83**, 641–671.
Ffowcs Williams, J. E. & Kempton, A. J. 1978 *J. Fluid Mech.* **84**, 673–694.
Moore, C. J. 1977 *J. Fluid Mech.* **80**, 321–367.
Moore, D. W. & Saffman, P. G. 1975 *J. Fluid Mech.* **69**, 465–473.
Munt, R. M. 1977 *J. Fluid Mech.* **83**, 609–640.
Pinker, R. A. & Bryce, W. D. 1977 *A.I.A.A. J.* **15**, 133–134.
Winant, C. D. & Browand, F. K. 1974 *J. Fluid Mech.* **63**, 237–255.
Wyber, R. J. 1975 *I.E.E.E. Trans. ASSP*-**23**, 157–162.

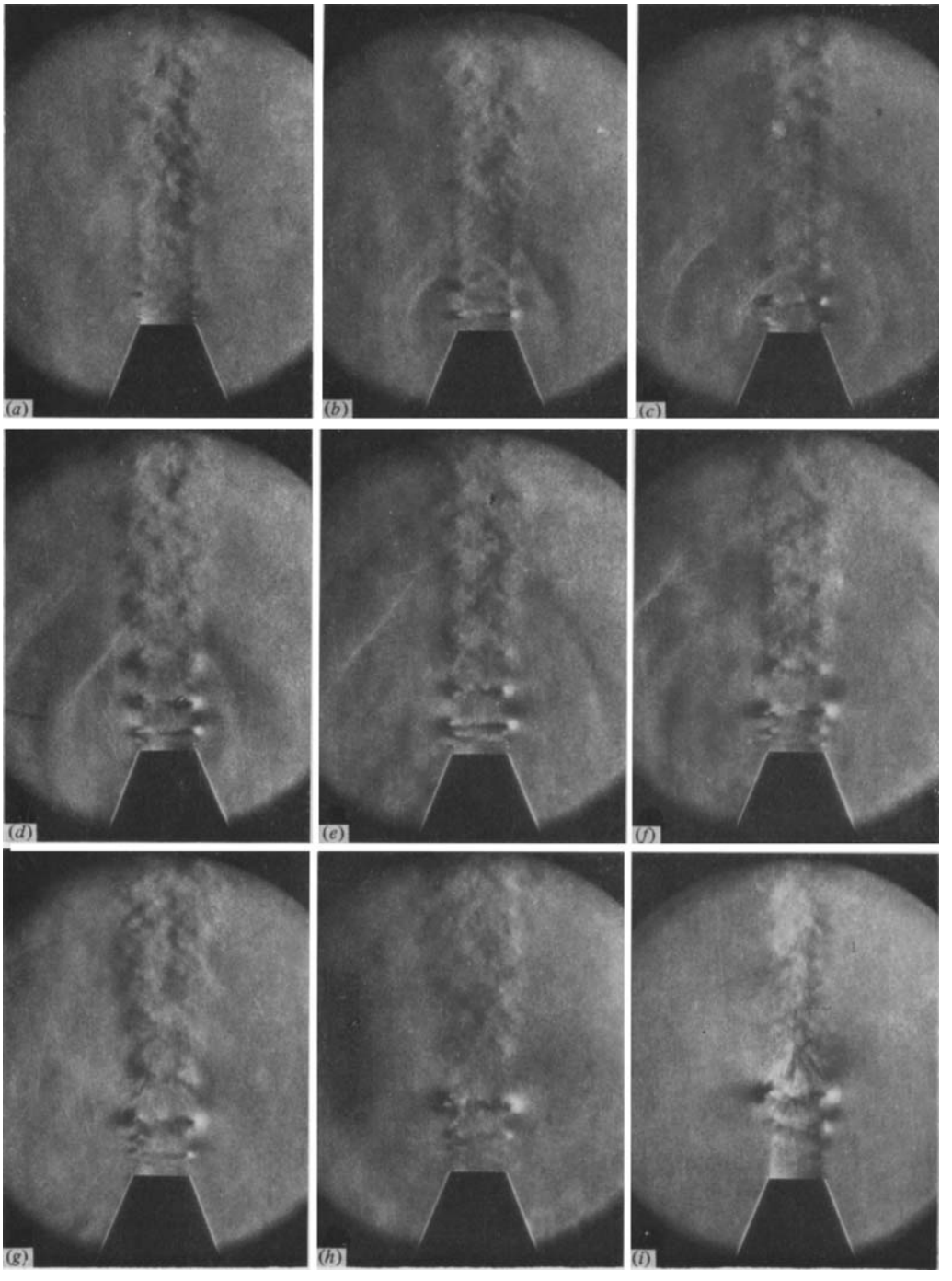

FIGURE 2. Sound diffraction and vortex generation in a Mach 0·6 jet excited by the N wave from a spark discharge. Schlieren knife edge vertical. Time interval between successive frames 33 μs.

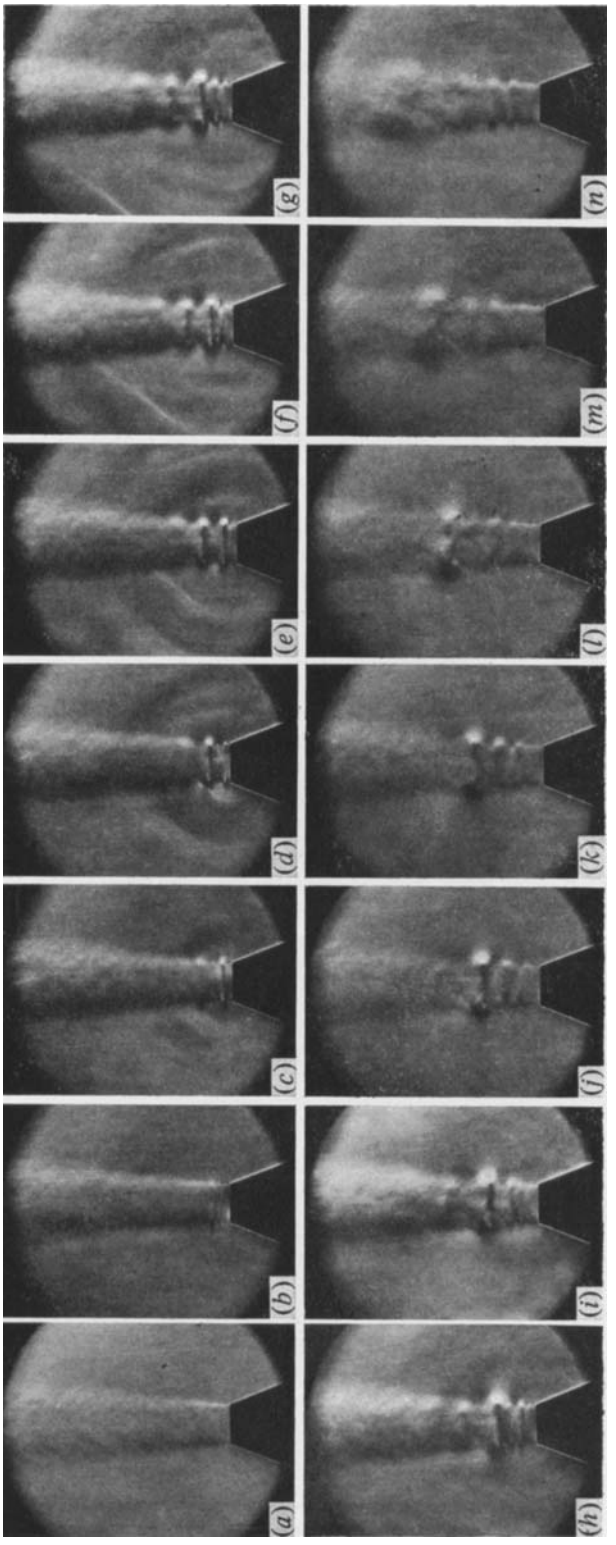

FIGURE 4. Multiple exposure photographs (10 exposures per frame) of the excited Mach 0·6 jet, showing the well-defined vortex-ring structure. Knife edge vertical, frame interval 33 μs.

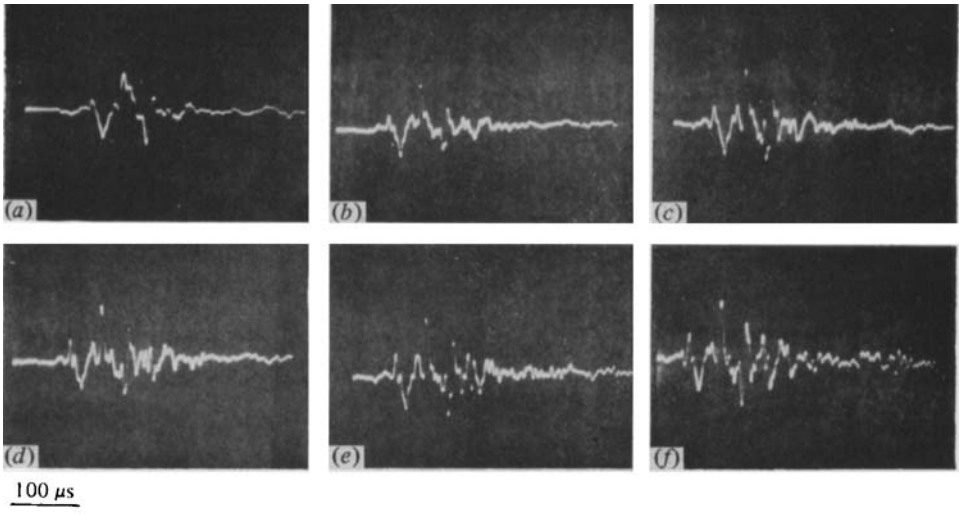

FIGURE 5. Measurement of the diffracted acoustic pulse at 90° to the jet axis (pressure is positive in the downward direction). Nozzle exit Mach number: (*a*) 0; (*b*) 0·44; (*c*) 0·53; (*d*) 0·60; (*e*) 0·66; (*f*) 0·77. Intensification is observed at the higher jet velocities.

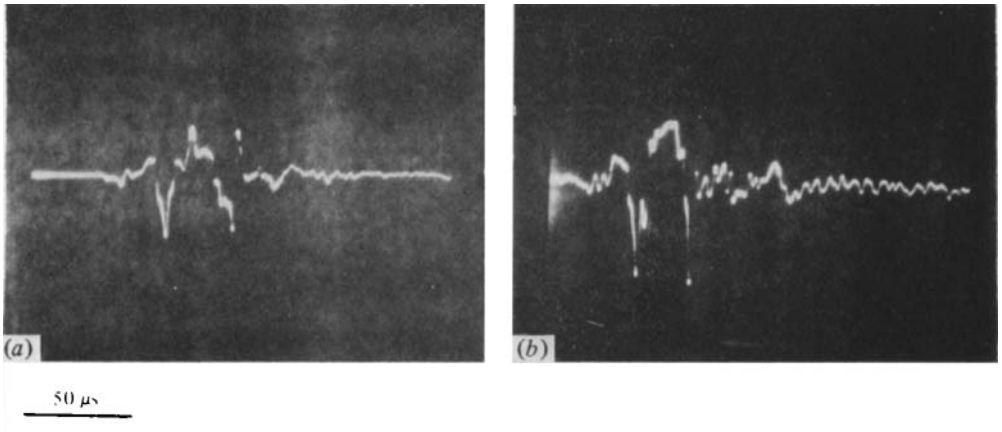

FIGURE 6. Measurement of the diffracted acoustic pulse at 45° to the jet axis. Nozzle exit Mach number: (*a*) 0; (*b*) 0·77.

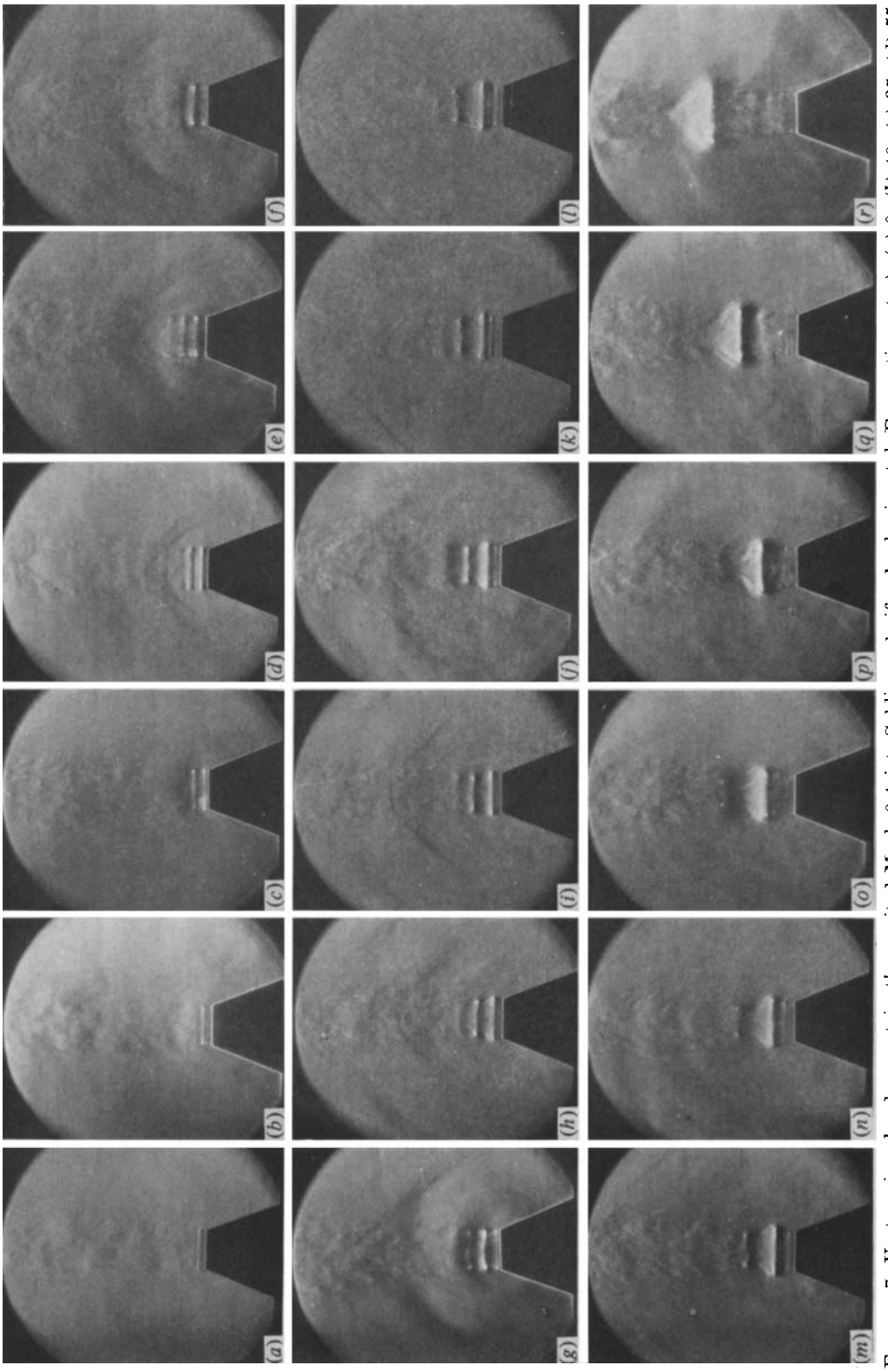

FIGURE 7. Vortex-ring development in the excited Mach 0·4 jet. Schlieren knife edge horizontal. Frame times (μs): (*a*) 0; (*b*) 10; (*c*) 35; (*d*) 55; (*e*) 75; (*f*) 95; (*g*) 110; (*h*) 140; (*i*) 155; (*j*) 180; (*k*) 210; (*l*) 220; (*m*) 230; (*n*) 240; (*o*) 280; (*p*) 320; (*q*) 420; (*r*) 580. Vortex coalescence occurs in frame (*m*).

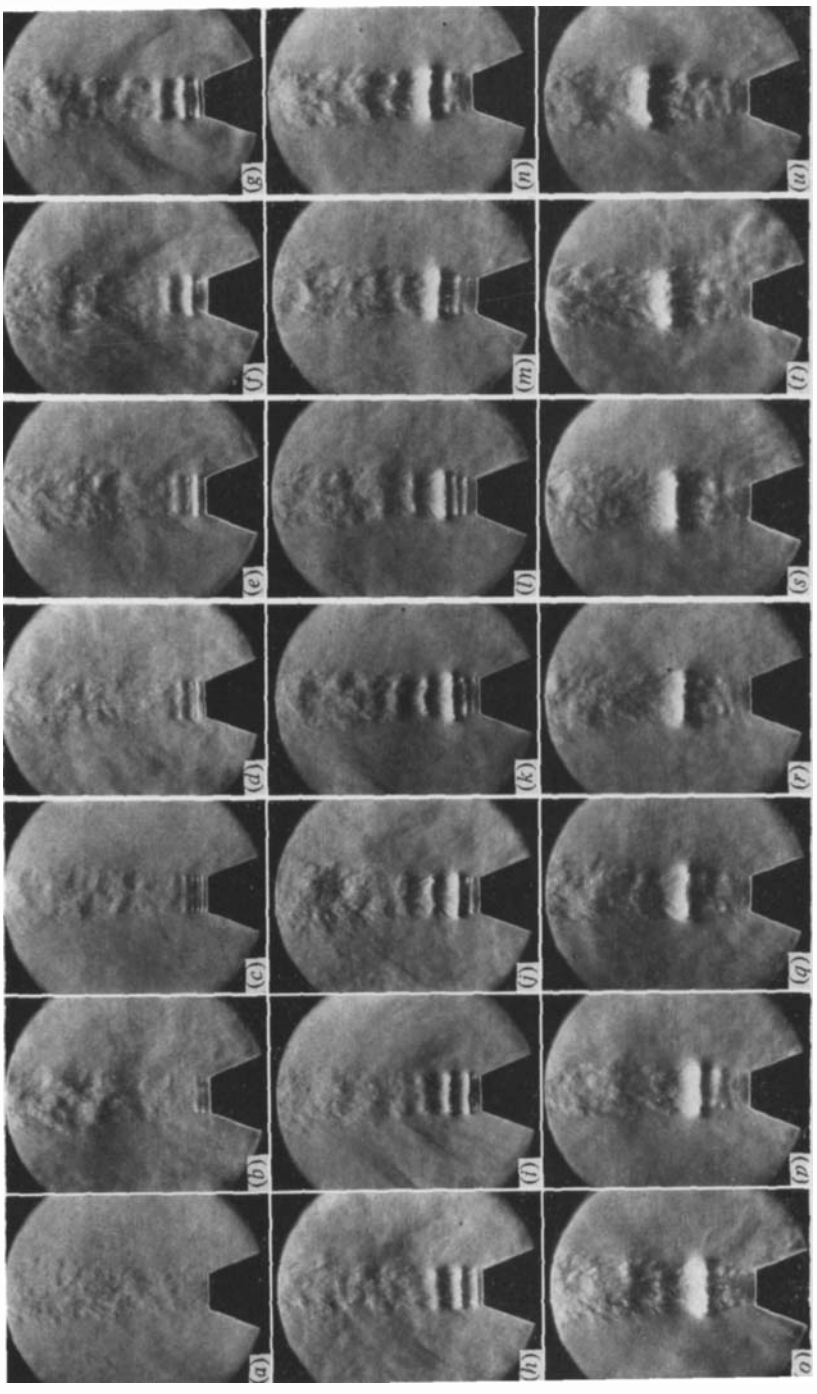

FIGURE 8. Vortex-ring development in the Mach 0·6 jet. Knife edge horizontal. Frame times (μs): (*a*) 0; (*b*) 30; (*c*) 45; (*d*) 55; (*e*) 70; (*f*) 100; (*g*) 110; (*h*) 120; (*i*) 150; (*j*) 195; (*k*) 220; (*l*) 230; (*m*) 240; (*n*) 295; (*o*) 325; (*p*) 340; (*q*) 390; (*r*) 410; (*s*) 435; (*t*) 460; (*u*) 515. Vortex coalescence occurs in frames (*d*), (*e*), (*h*), (*j*) and (*m*).

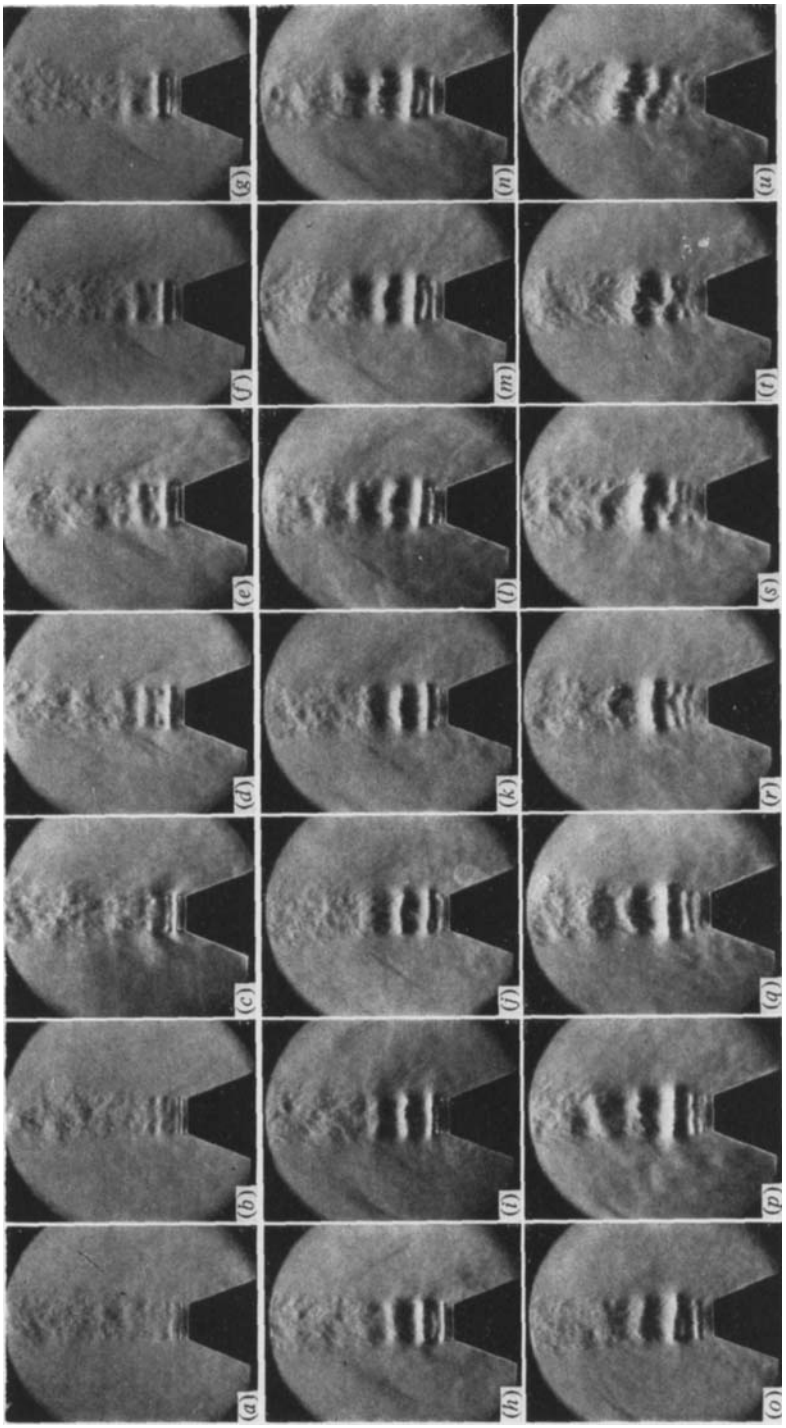

FIGURE 9. Vortex-ring development in the Mach 0·8 jet. Knife edge horizontal. Frame times (μs): (*a*) 0; (*b*) 35; (*c*) 65; (*d*) 85; (*e*) 95; (*f*) 100; (*g*) 110; (*h*) 135; (*i*) 150; (*j*) 160; (*k*) 170; (*l*) 195; (*m*) 205; (*n*) 215; (*o*) 230; (*p*) 240; (*q*) 250; (*r*) 290; (*s*) 305; (*t*) 325; (*u*) 350. Vortex coalescence occurs in frames (*e*), (*h*), (*i*), (*j*) and (*o*).

FIGURE 13. Near-field microphone signals from the pulse-excited Mach 0·6 jet recorded at various distances from the nozzle exit. Axial stations x/D: (*a*) 0; (*b*) 0·2; (*c*) 0·3; (*d*) 0·4; (*e*) 0·5; (*f*) 0·6; (*g*) 0·7; (*h*) 0·8; (*i*) 0·9; (*j*) 1·0; (*k*) 1·1; (*l*) 1·2; (*m*) 1·4; (*n*) 1·6; (*o*) 1·8.

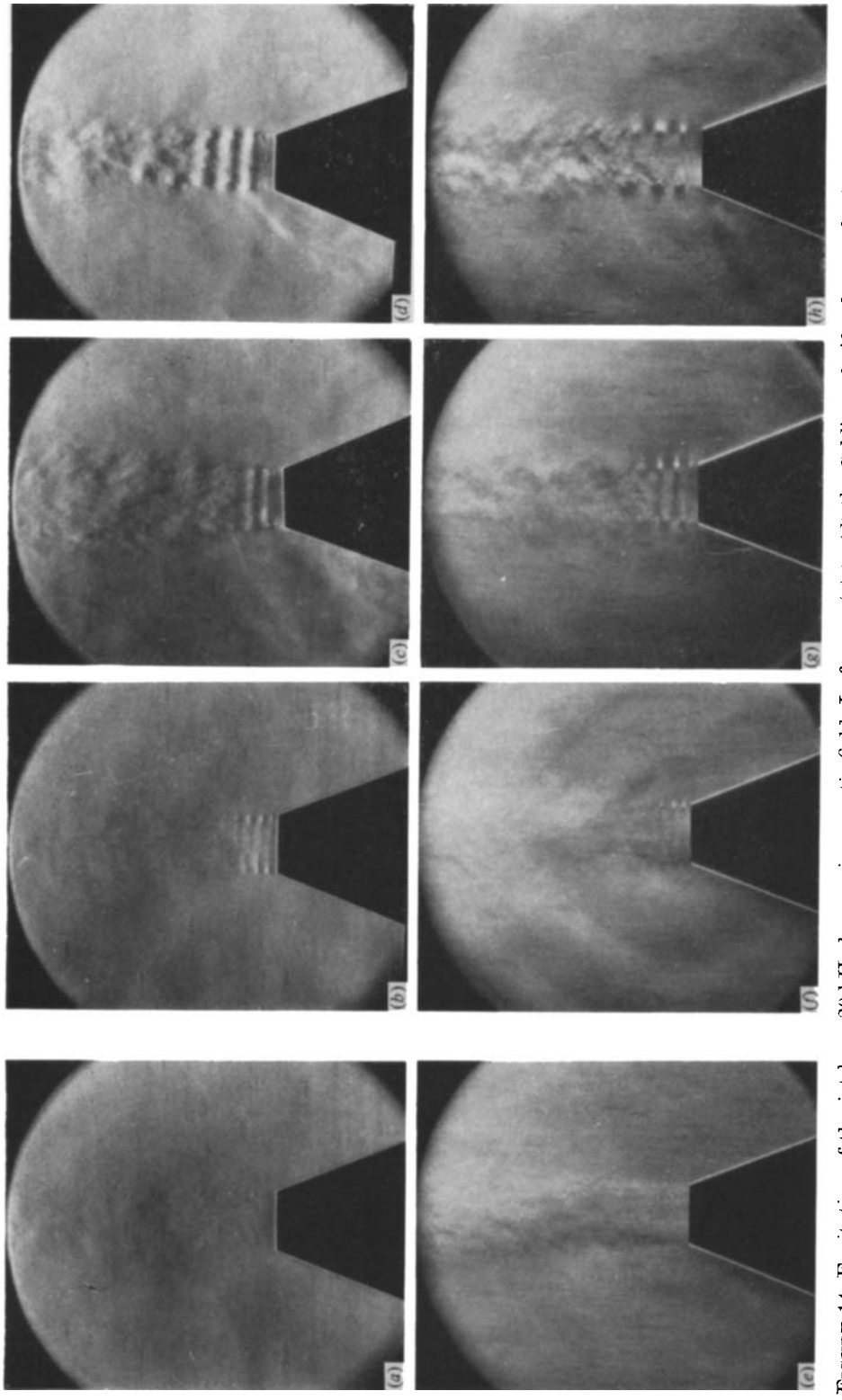

FIGURE 14. Excitation of the jet by a 20 kHz harmonic acoustic field. In frames (*a*) to (*d*) the Schlieren knife edge was horizontal; in frames (*e*) to (*h*) the knife edge was vertical. Frames (*a*) and (*e*) show an unforced Mach 0·3 jet. Forced-jet Mach numbers: (*b*), (*f*) 0·3; (*c*), (*g*) 0·45; (*d*), (*h*) 0·6. In these photographs the excitation level was kept constant.